

Nonlinear Field Equations for Aligning Self-Propelled Rods

Anton Peshkov,^{1,2,3} Igor S. Aranson,^{4,3} Eric Bertin,^{5,3} Hugues Chaté,^{1,2,3} and Francesco Ginelli⁶

¹*Service de Physique de l'Etat Condensé, CEA-Saclay, URA 2464 CNRS, 91191 Gif-sur-Yvette, France*

²*LPTMC, CNRS-UMR 7600, Université Pierre et Marie Curie, 75252 Paris, France*

³*Max Planck Institute for the Physics of Complex Systems, Nöthnitzer Strasse 38, 01187 Dresden, Germany*

⁴*Materials Science Division, Argonne National Laboratory, 9700 South Cass Avenue, Argonne, Illinois 60439, USA*

⁵*Université de Lyon, Laboratoire de Physique, ENS Lyon, CNRS, 46 Allée d'Italie, 69007 Lyon, France*

⁶*Institute for Complex Systems and Mathematical Biology, King's College, University of Aberdeen, Aberdeen AB24 3UE, United Kingdom*

(Received 24 July 2012; published 27 December 2012)

We derive a set of minimal and well-behaved nonlinear field equations describing the collective properties of self-propelled rods from a simple microscopic starting point, the Vicsek model with nematic alignment. Analysis of their linear and nonlinear dynamics shows good agreement with the original microscopic model. In particular, we derive an explicit expression for density-segregated, banded solutions, allowing us to develop a more complete analytic picture of the problem at the nonlinear level.

DOI: [10.1103/PhysRevLett.109.268701](https://doi.org/10.1103/PhysRevLett.109.268701)

PACS numbers: 87.18.Gh, 05.65.+b, 45.70.Vn

Collective motion is a central theme in the rapidly growing field of active matter studies which loosely groups together all situations where energy is spent locally to produce coherent motion [1]. In spite of the emergence of better-controlled, larger-scale experiments [2–6], our understanding of collective motion mostly comes from the study of mathematical models, and particularly of models of “dry” active matter systems, where the fluid which surrounds the moving objects can be neglected.

Microscopic models, then, usually consist of interacting self-propelled particles, as in the Vicsek model [7], where constant-speed point particles locally align their velocities. Their study, together with some more theoretical approaches, revealed a wealth of phenomena such as true long-range orientational order in two dimensions, spontaneous segregation of dense and ordered regions, anomalously strong number fluctuations, etc. [8–10].

These results have given rise to an emerging picture of universality classes, typically depending on the symmetries involved, which one would ideally characterize by some coarse-grained field equations. Different routes can be followed to obtain such equations: one can write *a priori* all terms allowed by symmetries up to some arbitrary order in gradients once hydrodynamic fields have been identified. One can also derive them from some microscopic starting point under more or less controlled and constraining assumptions, yielding more or less complete, well-behaved equations. There is, nevertheless, shared belief, based mostly on renormalization-group approaches, that in each case there exists a set of minimal equations accounting for all large-scale physics.

For polar particles aligning ferromagnetically (as in the Vicsek model), there is now near consensus about this minimal set of equations: the phenomenological theory initially proposed by Toner and Tu [11] is essentially

correct if one takes into account the dependencies of its coefficients on density and parameters initially overlooked but later derived from microscopic dynamics in Refs. [12,13]. It has been shown to reproduce many of the phenomena observed in microscopic models [14], although a complete study of its nonlinear solutions and dynamics is still lacking.

For the other important universality class of polar particles aligning *nematically*—e.g., self-propelled rods—the situation is less satisfactory: Baskaran and Marchetti [15] first derived rather lengthy yet mostly linear hydrodynamic equations for hard rods interacting via excluded volume, showing in particular the presence of global nematic, not polar, order, in agreement with microscopic observations [16]. Very recently [17], they added some nonlinear terms and performed a linear stability analysis of the homogeneous ordered state within an arbitrary choice of parameters. These even longer equations do not benefit from the same consensus as the Toner-Tu theory.

In this Letter, we derive a set of minimal nonlinear field equations describing the collective properties of self-propelled rods from a simple microscopic starting point, the Vicsek model with nematic alignment studied in Ref. [16]. We use a “Boltzmann-Ginzburg-Landau” approach, a controlled expansion scheme [18], which is a refined version of that used in Ref. [12]. Analysis of the solutions of these equations shows good agreement with the original microscopic model. In particular, we derive explicit expressions for density-segregated, banded solutions, allowing us to develop a more complete analytic picture of the problem at the nonlinear level.

In the Vicsek model with nematic alignment [16], point particles move off lattice at constant speed v_0 . Orientations and positions are updated following (here in two dimensions):

$$\theta_j^{t+1} = \arg \left[\sum_{k \sim j} \text{sign}[\cos(\theta_k^t - \theta_j^t)] e^{i\theta_k^t} \right] + \eta_j^t, \quad (1)$$

$$\mathbf{r}_j^{t+1} = \mathbf{r}_j^t + v_0 \mathbf{e}(\theta_j^{t+1}), \quad (2)$$

where $\mathbf{e}(\theta)$ is the unit vector along θ , the sum is taken over particles k within distance d_0 of particle j (including j itself), and η is a white noise with zero average and variance σ^2 . Like all Vicsek-style models, it shows orientational order at large-enough global density ρ_0 and/or small-enough noise strength σ . It was shown in Ref. [16] that the order is nematic and that both the ordered and disordered phases are subdivided in two: The homogeneous nematic phase observed at low noise is replaced at larger σ values by a segregated phase where a dense, ordered band occupying a fraction of space coexists with a disordered, dilute, gas. The transition to disorder is given by the onset of a long-wavelength instability of this band leading to a chaotic regime where bands constantly form, elongate, meander, and disappear over very long time scales. At still larger σ values, a “microscopically disordered” phase is observed.

Following Ref. [12], we write, in a dilute limit where only binary interactions are considered and assuming that orientations are decorrelated between them (“molecular chaos hypothesis”), a Boltzmann equation governing the evolution of the one-particle distribution $f(\mathbf{r}, \theta, t)$:

$$\partial_t f(\mathbf{r}, \theta, t) + v_0 \mathbf{e}(\theta) \cdot \nabla f(\mathbf{r}, \theta, t) = I_{\text{dif}}[f] + I_{\text{col}}[f], \quad (3)$$

with the angular diffusion and collision integrals

$$\begin{aligned} I_{\text{dif}}[f] &= -\lambda f(\theta) + \lambda \int_{-\pi}^{\pi} d\theta' f(\theta') \\ &\quad \times \int_{-\infty}^{\infty} d\eta P_{\sigma}(\eta) \delta_{2\pi}(\theta' - \theta + \eta), \\ I_{\text{col}}[f] &= -f(\theta) \int_{-\pi}^{\pi} d\theta' K(\theta', \theta) f(\theta') \\ &\quad + \int_{-\pi}^{\pi} d\theta_1 f(\theta_1) \int_{-\pi}^{\pi} d\theta_2 K(\theta_1, \theta_2) f(\theta_2) \\ &\quad \times \int_{-\infty}^{\infty} d\eta P_{\sigma}(\eta) \delta_{2\pi}(\Psi(\theta_1, \theta_2) - \theta + \eta), \quad (4) \end{aligned}$$

where $P_{\sigma}(\eta)$ is the microscopic noise distribution, $\delta_{2\pi}$ is a generalized Dirac delta imposing that the argument is equal to zero modulo 2π , $K(\theta_1, \theta_2) = 2d_0 v_0 |\mathbf{e}(\theta_1) - \mathbf{e}(\theta_2)|$ is the collision kernel for dilute gases [12], and $\Psi(\theta_1, \theta_2) = \frac{1}{2}(\theta_1 + \theta_2) + \frac{\pi}{2}[H[\cos(\theta_1 - \theta_2)] - 1]$ for $-\frac{\pi}{2} < \theta_2 - \theta_1 < \frac{3\pi}{2}$ [with $H(x)$ the Heaviside step function] codes for the nematic alignment. Rescaling of time, space, and density allows us to set the “collision surface” $S \equiv 2d_0 v_0 / \lambda = 1$ and $v_0 = 1$ below, without loss of generality.

Next, the distribution function is expanded in the Fourier series of the angle: $f(\mathbf{r}, \theta, t) = \frac{1}{2\pi} \sum_{k=-\infty}^{\infty} f_k(\mathbf{r}, t) e^{-ik\theta}$, with $f_k = f_{-k}^*$ and $|f_k| \leq f_0$. The zero mode is nothing

but the local density, while f_1 and f_2 give access to the polar and nematic order parameter fields \mathbf{P} and \mathbf{Q} :

$$\begin{aligned} \rho &= f_0, & \rho \mathbf{P} &= \begin{pmatrix} \text{Re} f_1 \\ \text{Im} f_1 \end{pmatrix}, \\ \rho \mathbf{Q} &= \frac{1}{2} \begin{pmatrix} \text{Re} f_2 & \text{Im} f_2 \\ \text{Im} f_2 & -\text{Re} f_2 \end{pmatrix}. \end{aligned} \quad (5)$$

As a matter of fact, it is convenient to use f_1 and f_2 , together with the “complex” operators $\nabla \equiv \partial_x + i\partial_y$ and $\nabla^* \equiv \partial_x - i\partial_y$. The continuity equation governing ρ is given by integrating the Boltzmann equation over angles:

$$\partial_t \rho + \text{Re}(\nabla^* f_1) = 0. \quad (6)$$

In Fourier space, the Boltzmann equation (3) yields an infinite hierarchy of equations:

$$\begin{aligned} \partial_t f_k + \frac{1}{2}(\nabla f_{k-1} + \nabla^* f_{k+1}) \\ = (\hat{P}_k - 1)f_k + \frac{2}{\pi} \sum_{q=-\infty}^{\infty} \left[\hat{P}_k J_{kq} - \frac{4}{1-4q^2} \right] f_q f_{k-q}, \end{aligned} \quad (7)$$

where $\hat{P}_k = \int_{-\infty}^{\infty} d\eta P_{\sigma}(\eta) e^{ik\eta}$ and

$$\begin{aligned} J_{kq} &= \int_{-\pi/2}^{\pi/2} d\phi \left| \sin \frac{\phi}{2} \right| e^{i((k/2)-q)\phi} + \cos \frac{k\pi}{2} \\ &\quad \times \int_{\pi/2}^{3\pi/2} d\phi \left| \sin \frac{\phi}{2} \right| e^{i((k/2)-q)\phi}. \end{aligned} \quad (8)$$

To truncate and close this hierarchy, we adopt the following scaling structure, valid near onset of *nematic* order, assuming, in a Ginzburg-Landau-like approach [18], small and slow variations of the density and of the polar and nematic fields:

$$\rho - \rho_0 \sim \epsilon, \quad \{f_{2k-1}, f_{2k}\}_{k \geq 1} \sim \epsilon^k, \quad \nabla \sim \epsilon, \quad \partial_t \sim \epsilon. \quad (9)$$

Note that the scaling of space and time is in line with the propagative structure of our system, as seen in the continuity equation (6), which contains no diffusion term.

The first nontrivial order yielding well-behaved equations is ϵ^3 : keeping only terms up to this order, equations for $f_{k>4}$ identically vanish, while those for f_3 and f_4 provide expressions of these quantities in terms of ρ , f_1 , and f_2 , which allows us to write the closed equations:

$$\begin{aligned} \partial_t f_1 &= -\frac{1}{2}(\nabla \rho + \nabla^* f_2) + \frac{\gamma}{2} f_2^* \nabla f_2 \\ &\quad - (\alpha - \beta |f_2|^2) f_1 + \zeta f_1^* f_2, \end{aligned} \quad (10)$$

$$\begin{aligned} \partial_t f_2 &= -\frac{1}{2} \nabla f_1 + \frac{\nu}{4} \nabla^2 f_2 - \frac{\kappa}{2} f_1^* \nabla f_2 - \frac{\chi}{2} \nabla^*(f_1 f_2) \\ &\quad + (\mu - \xi |f_2|^2) f_2 + \omega f_1^2 + \tau |f_1|^2 f_2, \end{aligned} \quad (11)$$

where all coefficients depend only on the noise strength σ (via the \hat{P}_k coefficients) and the local density ρ :

$$\begin{aligned}
\nu &= \left[\frac{136}{35\pi} \rho + 1 - \hat{P}_3 \right]^{-1} & \omega &= \frac{8}{\pi} \left[\frac{1}{6} - \frac{\sqrt{2}-1}{2} \hat{P}_2 \right] \\
\mu &= \frac{8}{\pi} \left[\frac{2\sqrt{2}-1}{3} \hat{P}_2 - \frac{7}{5} \right] \rho - 1 + \hat{P}_2 & \zeta &= \frac{8}{5\pi} \\
\alpha &= \frac{8}{\pi} \left[\frac{1}{3} - \frac{1}{4} \hat{P}_1 \right] \rho + 1 - \hat{P}_1 & \chi &= \nu \frac{2}{\pi} \left[\frac{4}{5} + \hat{P}_3 \right] \\
\kappa &= \nu \frac{8}{15} \left[\frac{19}{7} - \frac{\sqrt{2}+1}{\pi} \hat{P}_2 \right] & \gamma &= \nu \frac{4}{3\pi} \left[\hat{P}_1 - \frac{2}{7} \right] \\
\tau &= \chi \frac{8}{15} \left[\frac{19}{7} - \frac{\sqrt{2}+1}{\pi} \hat{P}_2 \right] & \beta &= \gamma \frac{2}{\pi} \left[\frac{4}{5} + \hat{P}_3 \right] \\
\xi &= \frac{32}{35\pi} \left[\frac{1}{15} + \hat{P}_4 \right] \left[\frac{13}{9} - \frac{6\sqrt{2}+1}{\pi} \hat{P}_2 \right] \\
&\times \left[\frac{8}{3\pi} \left(\frac{31}{21} + \frac{\hat{P}_4}{5} \right) \rho + 1 - \hat{P}_4 \right]^{-1}. \tag{12}
\end{aligned}$$

Below, for convenience, we choose the Gaussian noise distribution $P_\sigma(\eta) = \frac{1}{\sigma\sqrt{2\pi}} \exp[-\frac{\eta^2}{2\sigma^2}]$ for which $\hat{P}_k = \exp[-\frac{1}{2}k^2\sigma^2]$ [19]. A few remarks are, then, in order. First, μ can change sign and become positive for large enough ρ , while α is always positive. The homogeneous disordered state ($f_1 = f_2 = 0$) undergoes an instability to nematic order when $\mu = 0$, defining the basic transition line $\sigma_t(\rho_0)$ in the (ρ_0, σ) plane [Fig. 1(a)]. Next, ξ being positive in the $\mu > 0$ region where the disordered solution is unstable, Eqs. (10) and (11) possess a homogeneous nematically ordered solution $(f_1, f_2) = (0, \sqrt{\mu/\xi})$ (assuming order along \mathbf{x} , so that f_2 is real positive) [20]. The nonlinear terms express the complicated relation between the polar and nematic fields, which are both slow modes. In particular, nonlinearities in Eq. (10) do depend on f_2 and prevent the trivial exponential decay of f_1 , as predicted by

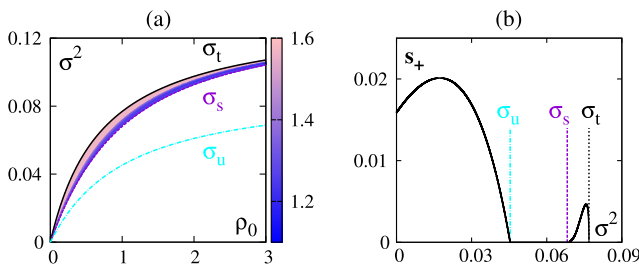


FIG. 1 (color online). (a) Linear stability of homogeneous solutions in the (ρ_0, σ) plane (plotted as a function of σ^2 to enhance clarity). The line $\rho = \frac{15\pi(\hat{P}_2-1)}{40\hat{P}_2(2\sqrt{2}-1)-64}$, given by $\mu = 0$, is the basic instability line defining $\rho_t(\sigma)$ or $\sigma_t(\rho_0)$: above it, the disordered homogeneous solution is linearly stable; below, it becomes unstable and the ordered solution $f_2 = \sqrt{\mu/\xi}$ exists. This solution is unstable between the σ_t and the σ_s lines. It is linearly stable between σ_s and σ_u , which marks the border of a region where $q = 0$ is the most unstable mode. The color scale codes for the angle between the most unstable wave vector and the direction of nematic order. (b) Largest eigenvalue s_+ (when positive) as a function of σ^2 for $\rho_0 = 1$.

linear theories [17], which would result in active nematic field equations [9]. On the other hand, the familiar nonlinearities of the Toner-Tu theory for polar systems may only be recovered if f_2 would get enslaved to f_1 [12], which is not possible in a system with nematic interactions where $\mu > 0$.

In the following, we further expand coefficients up to ϵ^3 in $\rho - \rho_0$, which amounts to keeping the crucial ρ dependence in μ and α and replacing ρ by ρ_0 in all other coefficients. This does not change any of our main results, but allows us to find exact band solutions (see below).

We have studied the linear stability of the homogeneous nematic solution with respect to perturbations of an arbitrary wave vector in the full (ρ_0, σ) parameter plane (Fig. 1). Similar to the polar case with ferromagnetic alignment [12–14,21], this solution is unstable to long wavelengths in a region bordering the basic transition line. The most unstable modes in this region are roughly—but not exactly—transversal to the order of the solution [22]. The homogeneous nematic solution becomes linearly stable deeper in the ordered phase [line σ_s in Fig. 1(a)], but its stability domain is limited by another instability region where $q = 0$ is the most unstable mode (line σ_u , which can be shown to be given by $\alpha + \zeta\sqrt{\mu/\xi} - \beta\mu/\xi = 0$). This strong instability, which occurs at large densities and/or weak noise, may be an artifact introduced by our truncation [24].

To go beyond the linear stability analysis of spatially homogeneous solutions, we performed numerical integrations of Eqs. (6), (10), and (11) in rectangular domains with periodic boundary conditions of typical linear sizes 50–200 [25]. For parameter values in the instability region of the nematic homogeneous solution, we observe stationary asymptotic solutions in which nematic order is confined to and oriented along a dense band with local density ρ_{band} amidst a homogeneous disordered “gas” with ρ_{gas} such that $\rho_{\text{band}} > \rho_s > \rho_t > \rho_{\text{gas}}$ [Fig. 2(a)], where $\rho_s(\sigma)$ is given by inverting $\sigma_s(\rho_0)$. Varying system size and using various domain aspect ratios, we find most often a single band oriented along the shortest dimension of the domain, which occupies a size-independent fraction Ω of space. All these observations are in agreement with the behavior of the original microscopic model [16].

Band solutions are also present *beyond* the region of instability of the homogeneous ordered state. Starting from, e.g., sufficiently inhomogeneous initial conditions, we find band solutions both for ρ_0 values larger than ρ_s , where they coexist with the homogeneous ordered phase, and below ρ_t , where the disordered homogeneous solution is linearly stable. Working at fixed ρ_0 varying σ for clarity, we thus find bands in a $[\sigma_{\text{min}}, \sigma_{\text{max}}]$ interval larger than the linear-instability interval $[\sigma_s, \sigma_t]$ (Fig. 3). Along it, the fraction occupied by the ordered band decreases from $\Omega \approx 1$ near σ_{min} to $\Omega \approx 0$ near σ_{max} . Furthermore, within a small layer $\sigma_{\text{max}} < \sigma \leq \sigma_c$, the bands are unstable, giving rise to a chaotic regime where they twist, elongate, break, and form again, in a manner strikingly similar to

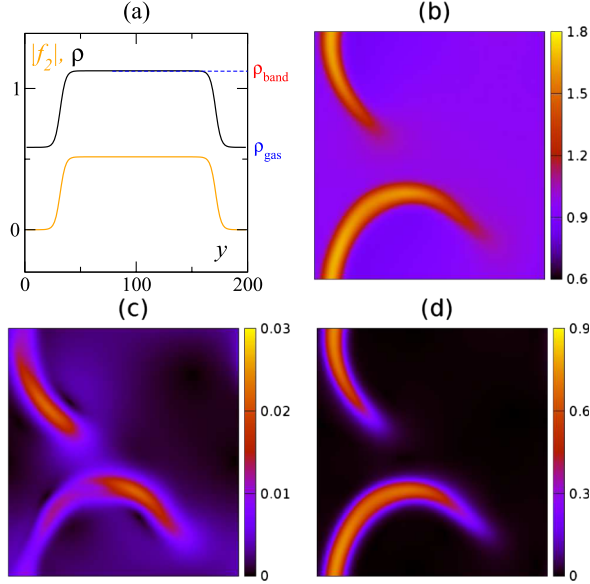


FIG. 2 (color online). Numerically obtained density-segregated solutions. (a) density and f_2 profiles of a stationary banded solution ($f_1 = 0$ throughout). The fronts linking the disordered and ordered domains can be perfectly fitted to hyperbolic tangents (not shown). ($\sigma = 0.26$, $\rho_0 = 1$, $L = 100$) (b, c, d) chaotic band regime: snapshots of (respectively) ρ , $|f_1|$, and $|f_2|$. ($\sigma = 0.2826$, $\rho_0 = 1$, $L = 200$).

observations made in the original microscopic model (Figs. 2(b)–2(d), [26]).

Thus the region of linear instability of the homogeneous ordered solution does *not* correspond to the existence (and stability) domain of band solutions, which is wider. In the original microscopic model, with its built-in fluctuations, coexistence of band solutions and homogeneous order has not been reported, but the homogeneous solution was found metastable near the threshold of emergence of bands where these appear “suddenly” [16]. At the other end of the band existence region, no coexistence was reported between band solutions and the homogeneous disordered state, suggesting that the latter is always driven to the former by intrinsic fluctuations. All this suggests that transitions found in the microscopic model do *not* correspond to the linear stability limits of homogeneous solutions of our *deterministic* continuous equations, pointing to a subcritical bifurcation scenario.

We now derive band solutions analytically. Suppose that, as observed, $f_1 = 0$ for band solutions and that f_2 is real and positive (i.e., nematic order is along x), and depends only on y . For a stationary solution, Eq. (10) then yields, after integration over y ,

$$\rho - f_2 - \frac{1}{2}\gamma f_2^2 = \tilde{\rho}, \quad (13)$$

where $\tilde{\rho}$ is a constant. This allows us to write Eq. (11), again looking for stationary solutions, in terms of f_2 only:

$$\frac{\nu}{4}\partial_{yy}f_2 = -\mu'f_2(\tilde{\rho} - \rho_t + f_2) + \left[\xi - \frac{\gamma}{2}\mu'\right]f_2^3, \quad (14)$$

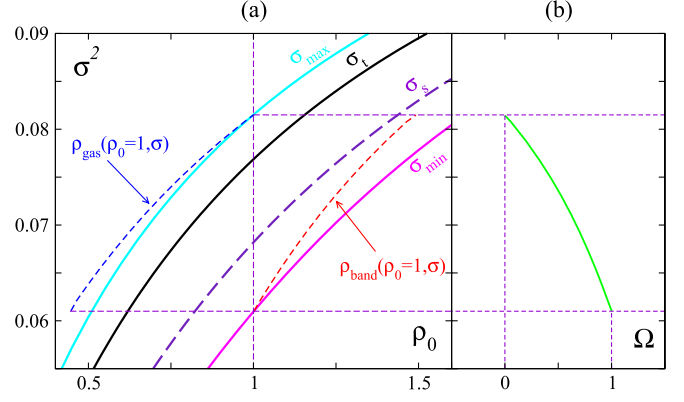


FIG. 3 (color online). Analytic band solutions for the slightly simplified system (see text). (a) (ρ_0, σ) parameter plane with basic instability line σ_t , stability limit of homogeneous ordered phase σ_s , and limits of existence of band solutions σ_{\min} and σ_{\max} . The short-dashed blue and red lines show the ρ_{gas} and ρ_{band} density values of the band solutions for $\rho_0 = 1$ as a function of σ over their existence range $[\sigma_{\min}, \sigma_{\max}]$, indicated by the thin horizontal dashed violet lines. (b) variation with σ of Ω , the fraction of space occupied by the ordered part of the band solution, for $\rho_0 = 1$.

where we have rewritten $\mu = \mu'(\rho - \rho_t)$, with μ' independent of ρ . Direct integration of Eq. (14) yields, under the condition $\lim_{y \rightarrow \pm\infty} f_2(y) = 0$, the following solution

$$f_2(y) = \frac{3(\rho_t - \tilde{\rho})}{1 + a \cosh(2y\sqrt{\mu'(\rho_t - \tilde{\rho})/\nu})}, \quad (15)$$

where $a = \sqrt{1 + 9b(\tilde{\rho} - \rho_t)/2\mu'}$ and $b = \xi - \mu'\gamma/2$. The value of $\tilde{\rho}$ can be obtained from the condition $\int_L \rho(y)dy = L\rho_0$, where L is the size of the box. We can neglect the exponentially decreasing tails in the integral and solve the equation $\int_{-\infty}^{\infty} [\rho(y) - \tilde{\rho}]dy = L(\rho_0 - \tilde{\rho})$. Under the assumption $L \rightarrow \infty$ we obtain

$$\tilde{\rho} \approx \rho_t - \frac{2\mu'}{9b}(1 - K_1 e^{-K_2 L}), \quad (16)$$

where K_1 and K_2 are positive quantities depending on σ and ρ_0 whose expression we omit for compactness. Substituting this value in the expression of a gives us $a = K_1 e^{-K_2 L/2}$, yielding a width of the band proportional to L , in agreement with observations on the microscopic model. As $L \rightarrow \infty$, the value of $\tilde{\rho}$ converges to the asymptotic value $\tilde{\rho}_{\text{gas}}$.

To determine the surface fraction Ω occupied by the ordered band, we use the relation $\Omega(\rho_{\text{band}} - \rho_{\text{gas}}) + \rho_{\text{gas}} = \rho_0$. Substituting the value of ρ_{band} obtained from Eqs. (13) and (15) at $y = 0$, we find for $L \rightarrow \infty$

$$\Omega = \frac{9b^2(\rho_0 - \rho_t) + 2b\mu'}{2\mu'(\gamma\mu' + 3b)}. \quad (17)$$

The condition $0 < \Omega < 1$ yields the lower limit σ_{\min} and the upper limit σ_{\max} of existence of the band solution.

Its stability will be analyzed in a forthcoming paper [27]. All these results are presented in Fig. 3.

To summarize, using a “Boltzmann-Ginzburg-Landau” controlled expansion scheme, we derived a set of minimal yet complete nonlinear field equations from the Vicsek model with nematic alignment studied in Ref. [16]. This simple setting allowed for a comprehensive analysis of the linear and nonlinear dynamics of the field equations obtained because our approach automatically yields a “meaningful manifold” parametrized by global density and noise strength in the high-dimensional space spanned by all coefficients of the continuous equations. Excellent agreement was found (at a qualitative level) with the simulations of the original microscopic model. The banded solutions were studied analytically. Their existence domain was found different from the region of linear instability of the homogeneous ordered phase, stressing the importance of a nonlinear analysis. More work, beyond the scope of this Letter, is needed to obtain a better understanding of the chaotic regimes observed. To this aim, we plan to study the linear stability of the band solutions in two dimensions.

Our equations (10) and (11) are simpler than those written by Baskaran and Marchetti in Refs. [15,17], not only because our microscopic starting point does not include positional diffusion of particles. The method used there seems intrinsically different, yielding more terms, many with a different structure from ours, while some of our nonlinear ones do not appear. It is not known yet whether the equations of Ref. [17] can also account for the nonlinear phenomena described above. Future work should explore this point in some detail.

Finally, experiments showed that microtubules displaced by a “carpet” of dynein motors move collectively and form large vortical structures [6]. It was shown that a Vicsek model with nematic alignment, but one in which the microscopic noise is colored, accounts quantitatively for the observed phenomena. Extending the approach followed here to this case is the subject of ongoing work.

We thank the Max Planck Institute for the Physics of Complex Systems, Dresden, for providing the framework of the Advanced Study Group “Statistical Physics of Collective Motion” within which much of this work was conducted. The work of I. S. A. was supported by the U.S. Department of Energy, Office of Basic Energy Sciences, Division of Materials Science and Engineering, under Contract No. DEAC02-06CH11357.

-
- [1] S. Ramaswamy, *Annu. Rev. Condens. Matter Phys.* **1**, 323 (2010).
 - [2] J. Deseigne, O. Dauchot, and H. Chaté, *Phys. Rev. Lett.* **105**, 098001 (2010); J. Deseigne, S. Léonard, O. Dauchot, and H. Chaté, *Soft Matter* **8**, 5629 (2012).
 - [3] V. Schaller, C. Weber, C. Semmrich, E. Frey, and A.R. Bausch, *Nature (London)* **467**, 73 (2010); V. Schaller, C. Weber, E. Frey, and A.R. Bausch, *Soft Matter* **7**, 3213 (2011); V. Schaller, C.A. Weber, B. Hammerich, E. Frey,

- and A.R. Bausch, *Proc. Natl. Acad. Sci. U.S.A.* **108**, 19 183 (2011).
- [4] H.P. Zhang, A. Béer, E.L. Florin, and H.L. Swinney, *Proc. Natl. Acad. Sci. U.S.A.* **107**, 13 626 (2010); X. Chen, X. Dong, A. Beer, H.L. Swinney, and H.P. Zhang, *Phys. Rev. Lett.* **108**, 148101 (2012).
- [5] A. Sokolov, I.S. Aranson, J.O. Kessler, and R.E. Goldstein, *Phys. Rev. Lett.* **98**, 158102 (2007).
- [6] Y. Sumino, K.H. Nagai, Y. Shitaka, D. Tanaka, K. Yoshikawa, H. Chaté, and K. Oiwa, *Nature (London)* **483**, 448 (2012).
- [7] T. Vicsek, A. Czirok, E. Ben-Jacob, I. Cohen, and O. Shochet, *Phys. Rev. Lett.* **75**, 1226 (1995).
- [8] J. Toner, Y. Tu, and S. Ramaswamy, *Ann. Phys. (Amsterdam)* **318**, 170 (2005).
- [9] S. Ramaswamy, R. A. Simha, and J. Toner, *Europhys. Lett.* **62**, 196 (2003); S. Mishra and S. Ramaswamy, *Phys. Rev. Lett.* **97**, 090602 (2006); H. Chaté, F. Ginelli, and R. Montagne, *Phys. Rev. Lett.* **96**, 180602 (2006).
- [10] H. Chaté, F. Ginelli, G. Grégoire, and F. Raynaud, *Phys. Rev. E* **77**, 046113 (2008); G. Grégoire and H. Chaté, *Phys. Rev. Lett.* **92**, 025702 (2004).
- [11] J. Toner, and Y. Tu, *Phys. Rev. Lett.* **75**, 4326 (1995); *Phys. Rev. E* **58**, 4828 (1998); J. Toner, *Phys. Rev. E* **86**, 031918 (2012).
- [12] E. Bertin, M. Droz, and G. Grégoire, *Phys. Rev. E* **74**, 022101 (2006); *J. Phys. A* **42**, 445001 (2009).
- [13] T. Ihle, *Phys. Rev. E* **83**, 030901 (2011).
- [14] S. Mishra, A. Baskaran, and M. C. Marchetti, *Phys. Rev. E* **81**, 061916 (2010).
- [15] A. Baskaran and M. C. Marchetti, *Phys. Rev. E* **77**, 011920 (2008); *Phys. Rev. Lett.* **101**, 268101 (2008).
- [16] F. Ginelli, F. Peruani, M. Bär, and H. Chaté, *Phys. Rev. Lett.* **104**, 184502 (2010).
- [17] A. Baskaran and M. C. Marchetti, *Eur. Phys. J. E* **35**, 95 (2012).
- [18] I. S. Aranson and L. S. Tsimring, *Phys. Rev. E* **71**, 050901 (2005); **74**, 031915 (2006).
- [19] For Gaussian noise, and other unimodal, centered noise distributions, most of the coefficients above do not change sign and are positive in the parameter region of interest.
- [20] Other homogeneous solutions with both f_1 and f_2 nonzero exist, but they are not observed in simulations, being either unphysical (having a modulus larger than f_0) and/or unstable.
- [21] A. Gopinath, M.F. Hagan, M.C. Marchetti, and A. Baskaran, *Phys. Rev. E* **85**, 061903 (2011).
- [22] This near-threshold instability is generically present in all dry active matter systems with metric interactions. See, e.g., Refs. [21,23].
- [23] A. Peshkov, S. Ngo, E. Bertin, H. Chaté, and F. Ginelli, *Phys. Rev. Lett.* **109**, 098101 (2012).
- [24] Simulations of Eqs. (6), (10), and (11) in this region lead to unbounded growth, whereas the original Vicsek model with nematic alignment shows no sign of instability.
- [25] We used a pseudospectral code with Euler time stepping ($\Delta t = 0.01$), with at least 400×400 Fourier modes on square domains of linear size $L = 200$.
- [26] Compare with Fig. 2(d) of Ref. [16]. See Supplemental Material at <http://link.aps.org/supplemental/10.1103/PhysRevLett.109.268701> for a movie, and compare with Supplemental Material movie of Ref. [16].
- [27] A. Peshkov *et al.* (to be published).